ANALYSIS OF TEMPERATURE- AND STRAIN RATE DEPENDENCE OF COMPRESSIVE FLOW STRESS OF AL_2O_3/YAG COMPOSITE AT 1773 TO 1973K

Shojiro Ochiai*, Kei Kuhara*, Yuushi Sakai*, Sohei Iwamoto*, Hiroshi Okuda*, Mototsugu Tanaka*, Masaki Hojo*, Yoshiharu Waku, Narihito Nakagawa**, Mitsuhiko Sato**, Toshihiro Ishikawa****

***Kyoto University, ****Ube Industries Ltd**

Keywords: *Al_2O_3/YAG composite; Flow stress; Stress-strain curve; Ultra high temperature; Strain rate; Modeling; Finite element analysis*

Abstract

Strain rate- and temperature dependences of compressive flow stress at ultra high temperatures of the Al_2O_3/YAG composite, fabricated by unidirectional solidification of eutectic composition, was analyzed by the finite element method and by the rule of mixtures based on the isostrain and isostress models. The spatial distribution of equivalent stress and strain rate in the steady state plastic deformation, arising from the heterogeneous microstructure, was revealed, and the experimentally measured flow stresses of the composite at the strain rate $2.8x10^{-6}$ to 10^{-4}/s in the temperature range of 1773 to 1973 K were described by the finite element analysis. The measured flow stress of the composite was lower than the value predicted by the isostrain model and higher than that predicted by the isostress model, due to the deviation of the regularity of the microstructure of the practical composite from that of the isostrain and isostress models.

1 Introduction

The directionally solidified eutectic oxide/oxide ceramic composite, such as a Al_2O_3/YAG (Yttrium-Aluminum Garnet with the composition of $Y_3A_{l5}O_{13}$), is one of the promising candidate materials to improve the thermal efficiency in jet aircraft engines and high-efficiency power-generation gas turbines [1-3], due to the following features. (i) The interface is clean without glassy phase [4-6]. (ii) The microstructure is very stable even when exposed at high temperatures in air. For instance, the microstructure does not vary even after exposure in air at 1973K for $3.6x10^3$ ks (1000h) [4]. (iii) The compressive creep strength at 1873K is about 13 times higher than that of the sintered composite with the same composition [5,7]. (iv) The flexural strength at room temperature, around 300-400 MPa, can be maintained almost up to the melting point of 2093K when the displacement speed is relatively high ($\approx 10^{-7}$ m/s) [4,5,8,9].

The study on macroscopic deformation behavior of the composite as a whole has revealed the excellence of this composite, as stated above. As the next step, the following problem shall be solved. The deformation and fracture behavior of this composite is sensitive to strain rate at ultra high temperature region above 1700 K [3,8-12]. As the composite is composed of Al_2O_3 and YAG with complicated shape (Fig.1 in which the dark and gray colors draw Al_2O_3 and YAG, respectively), the stress and strain rate are different from position to position. In order to reveal the correlation between the microstructure-dependent local stress state and the overall flow stress, the study on the microscopic spatial distribution of stress and strain rate at ultra high temperatures is requested.

The aim of the present work was (A) to describe the experimentally measured overall compressive flow stress of the composite at the strain rate $2.8x10^{-6}$ to 10^{-4} /s in the test temperature range of 1773 - 1973 K from the temperature- and strain rate-dependence of the constituting phases (Al_2O_3 and YAG), and (B) to reveal the stress and strain rate distribution in each phase. For the aim (A), the stress analysis was carried out by the finite element method (FEM) in which a model taken from the practical microstructure was used. Also the flow

stress calculation was carried by the rule of mixtures (ROM) based on the simple isostrain and isostress models. The calculation results were discussed in comparison with the experimental result. For the aim (B), the difference between the FEM- and ROM-calculated flow stress values was discussed, from which the influence of the geometrical deviation of the practical shape of the constituting phases from the regularity of the isostrain and isostress models on the overall flow stress was detected.

2 Experimental and modeling procedure

2.1 Sample and mechanical test se of Templates

The Al_2O_3/YAG composite with a eutectic composition was fabricated at Ube Industries Ltd., Yamaguchi, Japan, by the unidirectional solidification technique. Details of the fabrication method and micro-structural features are shown elsewhere [2-7]. The morphology is presented in Fig.1. The constituting phases are slightly elongated along the solidification direction.

The compression test of the composite specimens along the solidification direction was carried out at 1773, 1873 and 1973 K under the strain rate of $2.8\text{x}10^{-6}$, 10^{-5} and 10^{-4} /s in argon flow with the Instron-type machine (MTS 808) at Japan Ultra-high Temperature Materials Research Center. The size of the test specimens was 4x4 mm^2 in cross-section and 6 mm in height.

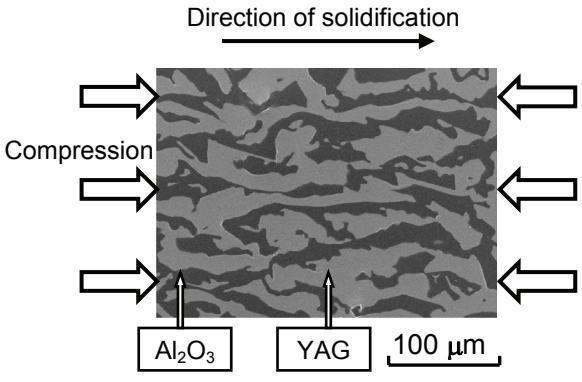

Fig.1 Polished cross-section parallel to the direction of solidification.

2.2 Finite element analysis

In our preceding work [12], it was attempted to describe the stress-strain behavior of the composite from the behavior of the constituting phases (Al_2O_3 and YAG) by the finite element analysis. The measured stress-strain curve consisting of elastic and plastic deformation regions of the composite at 1873K could be described satisfactorily. In this work, such a method was extended to describe the strain rate- and temperature dependence of the flow stress of the composite at the temperature range of 1773 to 1973K under the strain rate range of $2.8\text{x}10^{-6}$ to 10^{-4}/s. As details of the procedure have been reported in Ref.[12], the main items are picked up below.

As has been shown in Fig.1, the Al_2O_3 and YAG in the cross-section parallel to the solidification direction are elongated. For the finite element analysis, the two-dimensional model was taken from the observed microstructure, as shown in Fig.2. The model size was 0.3 mm in length along the loading direction (=solidification direction) and 0.15mm in width perpendicular to the loading direction. The boundary conditions are shown schematically in Fig.2(a). The analysis was carried out with the commercial finite element code MARC/Mentat™. In the calculation, the applied strain was raised in step of 0.0001. The Von Mises criterion was used as the criterion for yielding. After yielding, both Al_2O_3 and YAG were treated to deform plastically without strain hardening since the flow stress was nearly constant in the experimentally observed stress-strain curve as will be shown later in 3.1.

2.3 Calculation of flow stress as a function of strain rate and temperature based on the rule of mixtures

The rule of mixtures (ROM) of Young's modulus and coefficient of thermal expansion of unidirectional fiber-reinforced composite for the directions parallel and perpendicular to the fiber axis has been derived under the condition of the same axial strain (isostrain model (Fig.3(a)) and stress (isostress model (Fig.3(b)) for the fiber and matrix. As the microstructure of the present Al_2O_3/YAG composite is intermediate between the isostrain and isostress models, the flow stress of the composite is expected to fall in the range between the higher and lower bounds determined by the isostrain- and isostress models, respectively. If such an expectation is demonstrated to be valid at 1773-1973K, the simple rule of the mixtures can be a convenient tool to predict approximate bounds. The stress σ and strain rate $\dot{\varepsilon}$ in the plastic deformation range of composite, Al_2O_3 and YAG are expressed as $\sigma_c = \sigma_A V_A + \sigma_Y V_Y$ and $\dot{\varepsilon}_c = \dot{\varepsilon}_A = \dot{\varepsilon}_Y$ in the isostrain model,

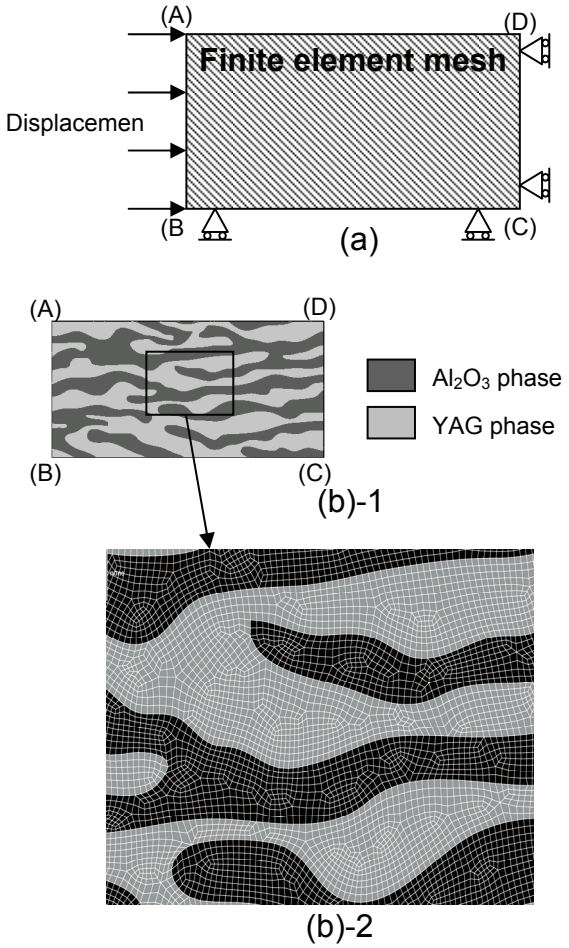

Fig.2 FEM model for stress analysis under compressive stress. (a) Boundary condition. (b)-1 observed configuration. (b)-2 Mesh. (Elements: 27312, Nodes: 27643).

and $\sigma_c = \sigma_A = \sigma_Y$ and $\dot{\varepsilon}_c = \dot{\varepsilon}_A V_A + \dot{\varepsilon}_Y V_Y$ in the isostress model, where V is the volume fraction (=0.5 for both Al_2O_3 and YAG in the present composite [5, 7]) and the subscripts c, A and Y refer to the composite, Al_2O_3 and YAG, respectively. Substituting the $\dot{\varepsilon}$ - T-σ relation of Al_2O_3 and YAG into these equations, the correlation of the flow stress of the composite to the applied strain rate and test temperature was calculated for both models.

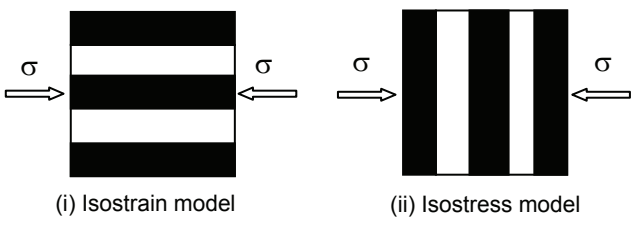

Fig.3 Isostrain and isostress models.

2.4 Input values

For calculation of flow stress of the composite, the following values were used commonly in the finite element analysis and the prediction by the rule of mixtures (isostrain and isostress models). The temperature (T) - dependences of the Young's modulus of Al_2O_3 and YAG were taken to be 423-0.0474T and 299-0.0180T GPa, respectively from Ref.[13]. The Poisson's ratio of Al_2O_3 and YAG was taken to be 0.23 and 0.25, respectively, from Ref.[14]. The temperature-dependences of the shear modulus of Al_2O_3 and YAG were taken to be 172-0.0193T and 120-0.0072T GPa, respectively, from Ref.[13]. It has been demonstrated in Ref.[13] that, with these property values of Al_2O_3 and YAG, the measured temperature dependence of Young's modulus of the composite is described.

As will be shown in 3.1, the steady state plastic deformation took place in the composite after yielding. In this region, the stress carrying capacity of Al_2O_3 and YAG is dependent on the strain rate $\dot{\varepsilon}$ and temperature T. The relation of the strain rate $\dot{\varepsilon}$ to flow stress σ in plastic deformation of Al_2O_3 and YAG was given by $\dot{\varepsilon} = A\sigma^n \exp(-Q/RT)$ where A is the constant, n the stress exponent, Q the activation energy for plastic deformation and R the gas constant). It has been shown in Ref.[8] that n=6 and Q=637 kJ/mol for Al_2O_3, taken from the reported data of Ref.[15], and n=6, Q=789 kJ/mol for YAG, taken from the reported data of Ref.[16], can account for the experimentally observed n and Q values of the composite. Thus, these values, together with $A=2.7\times10^{-2}$ and 1.3x10 ($s^{-1}MPa^{-6}$) for alumina and YAG, estimated from the reported data of Refs.[15] and [16], respectively, were used for calculation.

3 Results and discussion

3.1 Measured stress-strain curves, and strain rate- and temperature dependence of the flow stress of the composite

Examples of the measured stress-strain curve are presented in Fig.4. The flow stress in the plastic region is nearly constant, indicating that the steady state deformation occurs in the plastic region. In the present work, the stress at 1.5 % strain in the plastic region was taken as the flow stress. As the difference in the flow stress in the strain range of 1 to 3% was within a several percent, the stress taken at 2% strain was regarded as the common flow stress

in the plastic range. Figure 5 shows the strain rate – and temperature dependence of the flow stress. Evidently, the stress in the plastic region increases with increasing strain rate and decreasing temperature.

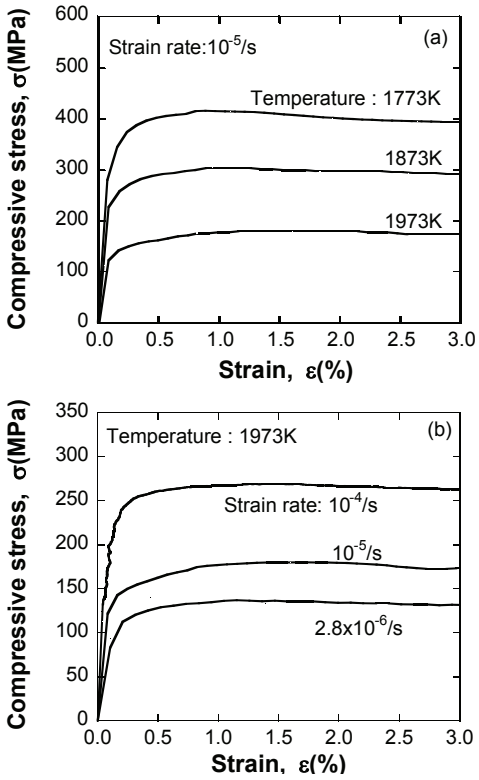

Fig.4 Measured stress-strain curves of the composite (a) at 1773, 1873 and 1973K under a strain rate of 10^{-5}/s and (b) at 1973K under the strain rates of 2.8×10^{-6}, 10^{-5} and 10^{-4}/s.

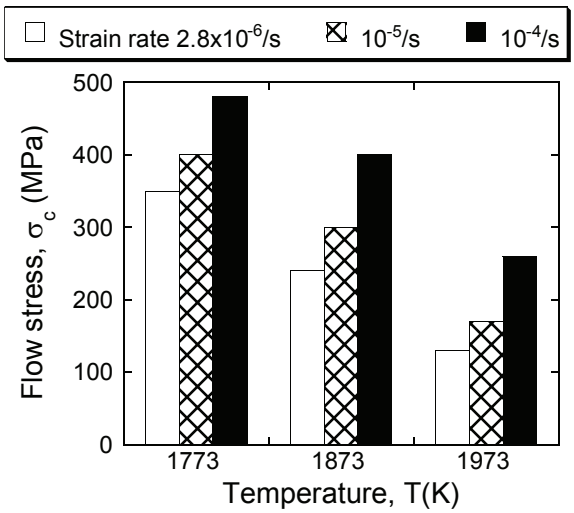

Fig.5 Measured flow stress of the composite in the steady state plastic deformation region.

In order to reveal the relation of the strain rate- and temperature dependence of the flow stress of the composite to that of the constituting phases, the experimental result shown in Fig.4 was analyzed by the finite element method and the rule of mixtures using the isostrain and isostress models, as shown below.

3.2 Comparison of FEM-calculated stress-strain curves with measured ones

Figure 6 shows the calculated stress-strain curves (a) at the temperatures 1773, 1873 and 1973K under a given strain rate 10^{-5}/s and (b) at the strain rates 2.8×10^{-6}, 10^{-5} and 10^{-4}/s under a given temperature 1973K. The measured stress-strain curves under the same conditions have been presented in Fig.4(a) and (b), respectively. The shape of the stress-strain curve and the flow stress level in the steady state plastic region shown in Fig.4 are fairly well reproduced in Fig.6. This result suggests that the model (Fig.2) and input values for calculation (mentioned in 2.4) were close to the practical ones.

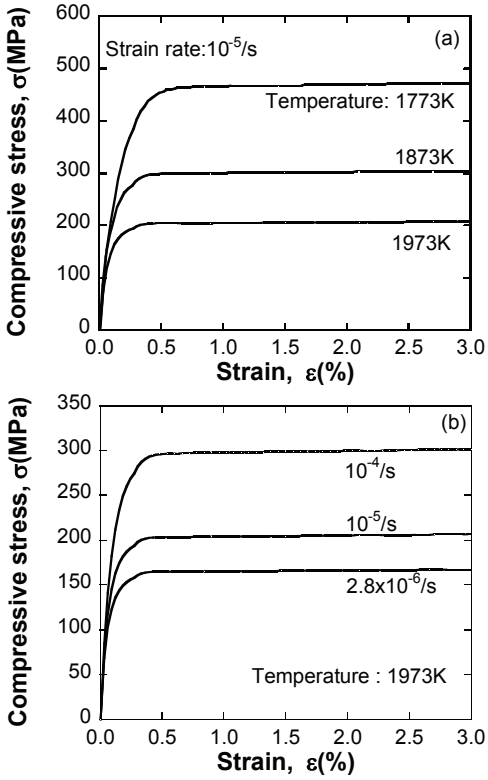

Fig.6 Calculated stress-strain curves (a) at 1773, 1873 and 1973K under a given strain rate 10^{-5}/s and (b) at 1973K under the strain rates of 2.8×10^{-6}, 10^{-5} and 10^{-4}/s.

3.3 Flow stress of composite

It was examined whether the flow stresses calculated by FEM can describe the experimental ones in the whole range of strain rate ($2.8x10^{-6}$ to 10^{-4}/s) and temperature (1773 to 1973 K) or not. Also it was examined whether the rule of mixtures (ROM), whose calculation method has been shown in 2.3, can give the approximate prediction of flow stress or not.

When the relation of the strain rate $\dot{\varepsilon}$ to flow stress σ in plastic deformation is given by the form, $\dot{\varepsilon} = A\sigma^n \exp(-Q/RT)$, the relation of $\ln(\sigma)$ to 1/T (inverse temperature) is linear. Thus it is convenient to use the $\ln(\sigma)$ - 1/T relation for comparison of the temperature-dependence of the flow stress of the composite with that of the constituents at a given strain rate. The measured flow stress-values of the composite and the calculated ones by FEM and ROM, together with the flow stress-values of the Al_2O_3 and YAG for reference, were superimposed in the $\ln(\sigma)$ - 1/T relation, as shown in Fig.7.

The experimental results in the whole range of strain rate ($2.8x10^{-6}$ to 10^{-4} /s) and temperature (1773 to 1973 K) are described fairly well by the FEM analysis. It is noted that the experimental flow stress values of composite are in the range between the lower bound given by ROM for isostress model and the upper one given by ROM for isostrain model. The reason for this is attributed to the deviation of the microstructure of the practical composite (Fig.1) from the regularity assumed in the isostrain and isostress models (Fig.3). Namely, due to the coexistence of the isostrain and isostress type morphologies within the composite, the flow stress is, to some extent, lower than the prediction of the isostrain model and higher than that of the isostress model. This suggests that, when the composite is stressed along the direction perpendicular to the solidification, the flow stress is lower than the present case due to the less amount of isostrain type morphology in the stress direction but never falls to the value predicted by the isostress model. Such a phenomenon has actually been observed [7,8,12].

It is noted that, while the isostrain and isostress models cannot describe the flow stress of the composite due to the coexistence of isostrain and isostress type morphologies, they can be a useful tool to predict the upper and lower bounds to a first approximation, since the difference between the lower and upper bounds given by these models is smaller than that of the flow stress values of the constituents (Al_2O_3 and YAG).

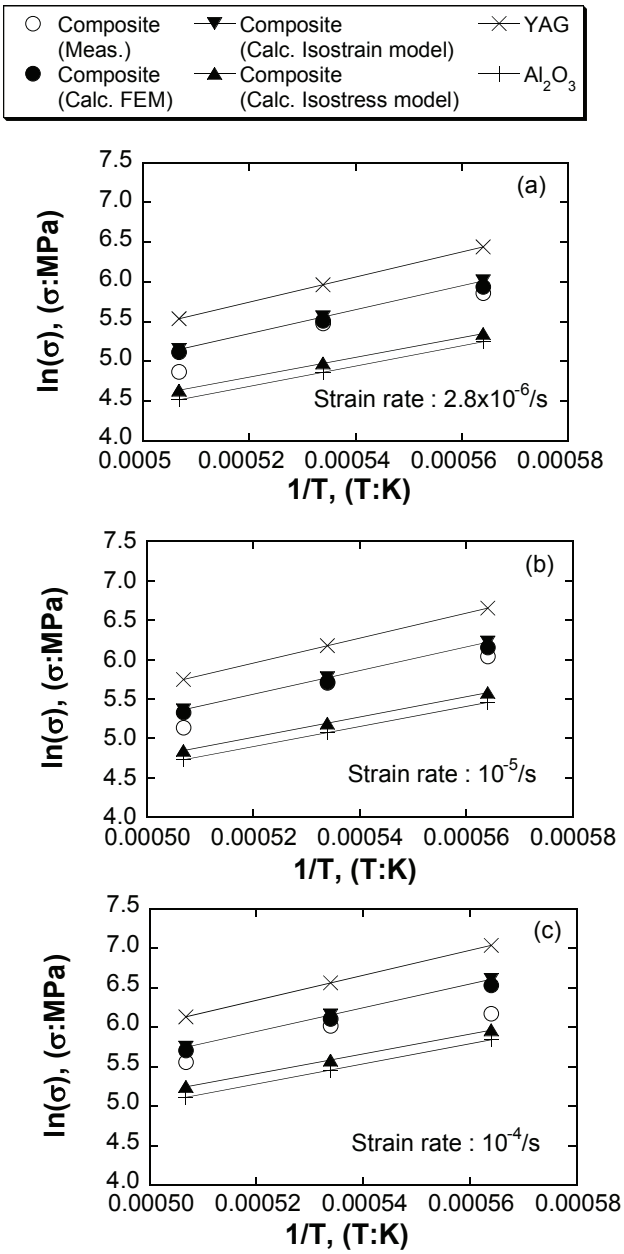

Fig.7 Comparison of the stress ($\ln(\sigma)$)-inverse temperature(1/T) relation among (○) measured flow stress of the composite, (●)FEM-calculated flow stress of the composite, (▼) isostrain model-calculated flow stress of the composite, (▲) isostress model-calculated flow stress of the composite, (×) flow stress of the monolithic YAG and (+) flow stress of the monolithic Al_2O_3 under the strain rate of (a) $2.8x10^{-6}$, (b) 10^{-5} and (c) 10^{-4}/s.

3.4 Stress and strain rate distribution in the plastic region

As shown above, the flow stress of the present composite is very sensitive to strain rate. If the structure is regular as in the isostrain and isostress models (Fig.3), the strain rate (stress) distribution shall be uniform to a first approximation. However, it is not the present case since Al_2O_3 and YAG form complex geometry in the present composite (Fig.1). Figures 8 and 9 show the calculated spatial distribution of equivalent stress and equivalent strain rate under the condition of applied strain 1.5%, strain rate 10^{-5}/s and temperature at 1773 and 1993 K, respectively. Evidently, the strain rate and the stress are distributed spatially even after overall yielding of the composite due to the micro structural deviation from regularity. Three features are read from the results in Figs.8 and 9. (i) The strain rate (stress) is concentrated in thick parts of Al_2O_3 and thin parts of YAG especially near the geometrical irregularities at any temperature. (ii) The strain rate distribution in Al_2O_3 is wider than that in YAG.. This result is accounted for by the softer nature of Al_2O_3.; the softer Al_2O_3 needs larger change in strain rate more than the harder YAG for the stress balance. (iii) The stress level at 1973K is quite different from that at 1773K. On the other hand, the strain rate distribution in Al_2O_3 and YAG at 1973K is similar to that at 1773K. Namely, the microstructural irregularity -induced stress is accommodated by the similar spatial distribution of strain rate within the temperature range investigated.

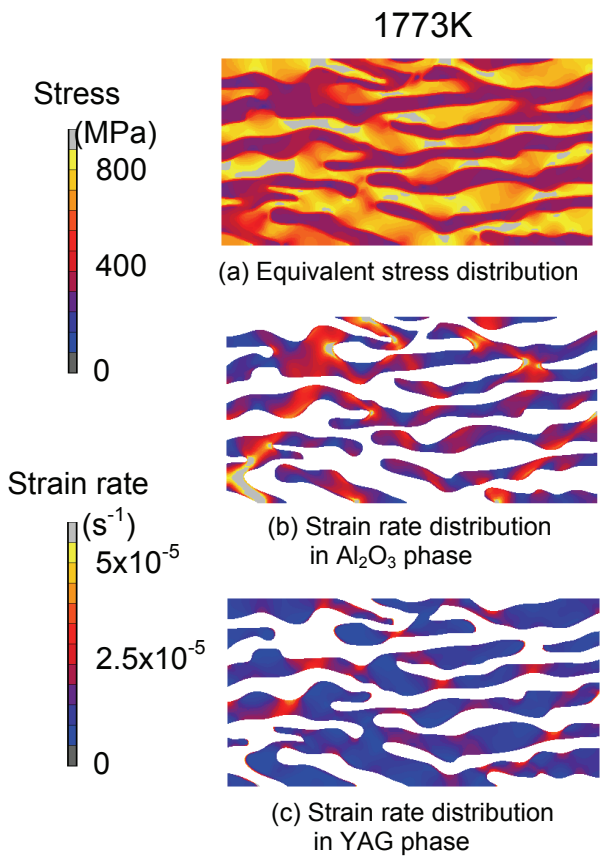

Fig.8 (a) Equivalent stress distribution in composite, and equivalent plastic strain rate distribution in (b) Al_2O_3 and (c) YAG phases at a strain rate of 10^{-5}/s at 1773 K.

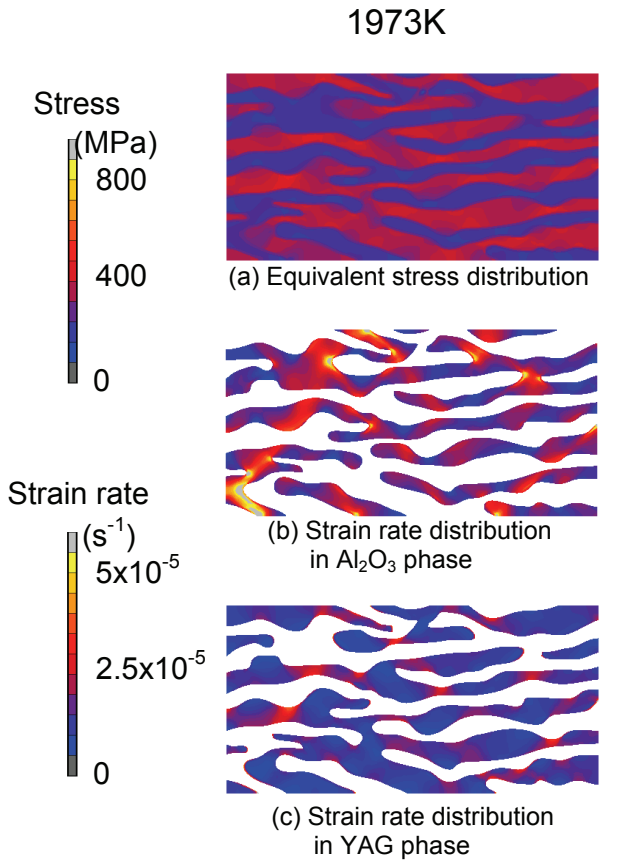

Fig.9 (a) Equivalent stress distribution in composite, and equivalent plastic strain rate distribution in (b) Al_2O_3 and (c) YAG phases at a strain rate of 10^{-5}/s at 1973 K.

4. Conclusions

(1) The measured stress-strain curve and flow stress of the directionally solidified Al_2O_3/YAG composite, deformed perpendicularly to the solidification direction at 1773 to 1973K under the strain rate range of 2.8×10^{-6} to 10^{-4}/s, were accounted for by the present finite element analysis, in which the temperature- and strain

rate dependence of the behavior of the Al_2O_3 and YAG.

(2) The rule of mixtures derived from the isostrain and isostress models could give the upper and lower bounds for the flow stress of the composite, respectively, which could be used for rough prediction of flow stress of this composite at ultra high temperatures.

(3) The spatial distribution of equivalent stress and strain rate in the steady state plastic deformation, arising from the heterogeneous microstructure was revealed. Following features were found. (i) The strain rate (stress) is concentrated in thick parts of Al_2O_3 and thin parts of YAG at any temperature and at any applied strain rate. (ii) The strain rate distribution in Al_2O_3 is wider than that in YAG. Due to the softer nature of Al_2O_3. (iii) Within the temperature range of 1773 to 1973K, the heterogeneous microstructure-induced stress is accommodated by the similar spatial distribution of strain rate.

References

[1] Hirano K. "Application of eutectic composites to gas turbine system and fundamental fracture properties up to 1700 °C". *J. Europ. Ceram. Soc.* Vol.25. No.8, pp. 1191-1199, 2005.

[2] Nakagawa N., Ohtsubo H., Mitani A., Shimizu K. and Waku Y. "High temperature strength and thermal stability for melt growth composite". *J. Europ. Ceram. Soc.* Vol.25. No.8, pp. 1251-1257, 2005.

[3] Llorca J. and Orera V. M. "Directionally solidified eutectic ceramic oxides", *Prog. Mater. Sci.,* Vol.51, pp.711-809, 2006.

[4] Waku Y., Nakagawa N., Otsubo H., Ohsora Y. and Kohtoku Y. "High temperature properties of unidirectionally solidified Al_2O_3/YAG composites". *J Japan Inst Metals* Vol.59, pp.71-78, 1995.

[5] Waku Y., Otsubo H., Nakagawa N. and Kohtoku Y. "Sapphire matrix composites reinforced with single crystal YAG phases". *J. Mater. Sci.* Vol.31, pp. 4663-4670, 1996.

[6] Waku Y., Nakagawa N., Wakamoto T., Otsubo H., Shimizu K. and Kohtoku Y. "High temperature strength and thermal stability of unidirectionally solidified Al_2O_3/YAG eutectic composite". *J. Mater. Sci.* Vol.33, pp.1217-1224, 1998.

[7] Waku Y., Nakagawa N., Wakamoto T., Otsubo H., Shimizu K. and Kohtoku Y. "The creep and thermal stability characteristics of a unidirectionally solidified Al_2O_3/YAG eutectic composite". *J. Mater. Sci.* Vol. 33; pp. 4843-4851, 1998.

[8] Yoshida H., Shimura K., Suginohara S., Ikuhara Y., Sakuma T., Nakagawa N. and Waku Y. "High-temperature deformation in unidirectionally solidified eutectic Al_2O_3-YAG single crystal". *Key Engng. Mater.* Vol.171-174; pp. 855-862, 2000.

[9] Ochiai S., Ueda T., Sato K., Hojo M., Waku Y., Nakagawa N., Sakata S., Mitani A. and Takahashi T. "Deformation and fracture behavior of Al_2O_3/YAG composite from room temperature to 2023K". *Compos. Sci .Technol.* Vol.61; pp. 2117-2128, 2001.

[10] Harada H., Suzuki T., Hirano K. and Waku Y. "Ultra-high temperature compressive creep behavior of an in-situ Al_2O_3 single-crystal/YAG eutectic composite". *J Europ Ceram Soc*., Vol.24, No.8, pp.2215-2222, 2004.

[11] Ochiai S., Sakai Y., Sato K., Tanaka M., Hojo M., Okuda H., Waku Y., Nakagawa N., Sakata S., Mitani, A. and Takahashi T. "Fracture Characteristics of Al_2O_3/YAG Composite at Room Temperature to 2023K", *J. Europ. Ceram. Soc.,* Vol.25, No.8, pp.1241-1249, 2005.

[12] Ochiai S., Sakai Y., Kuhara, K, Iwamoto, S., Okuda, H., Tanaka M., Hojo, M., Waku, Y., Nakagawa N., Sakata, S., Mitani, M., Sato, M. and Ishikawa, T. "Analytical modeling of stress-strain behavior at 1873K of alumina/YAG composite compressed parallel and perpendicular to the solidification direction", *Comp. Sci. Tecnol.*, Vol.67, No.2, pp.270-277, 2006.

[13] Ochiai S., Ueda T,. Sato K., Hojo M., Waku Y., Sakata S., Mitani A., Takahashi T. and Nakagawa N. "Elastic modulus and coefficient of thermal expansion of Al_2O_3/YAG composite at ultra high temperatures". *Mater. Sci. Res. Int. Special Technical Publication-2*, pp. 281-285, 2001.

[14] Waynant R. and Ediger M. "Electro-optics Handbook". Mcgrow-Hill Inc., pp. 11.13-11.23, 1994.

[15] Kotchick D. M. and Tressler R.E. "Deformation behavior of sapphire via the prismatic slip system". *J. Amer. Ceram. Soc.* Vol. 63; pp. 429-34, 1980.

[16] Corman G. S. "Creep of yttrium aluminium garnet single crystals". *J. Mater. Sci. Lett.* Vol. 12; pp. 379-82, 1993.